Character of 5*f* states in the Pu-Am system from magnetic susceptibility, electrical resistivity, and photoelectron spectroscopy measurements

N. Baclet,[1] M. Dormeval,[1] L. Havela,[2] J. M. Fournier,[3] C. Valot,[1] F. Wastin,[4] T. Gouder,[4] E. Colineau,[4] C. T. Walker,[4] S. Bremier,[4] C. Apostolidis,[4] and G. H. Lander[4]

[1]*Commissariat à l'Energie Atomique, CEA—Centre de Valduc, 21120 Is sur Tille, France*

[2]*Charles University, Faculty of Mathematics and Physics, Department of Condensed Matter Physics, Ke Karlovu 5, 121 16 Prague 2, Czech Republic*

[3]*Université Joseph Fourier LEG-INPG, BP46, 38402 Saint Martin d'Hères Cedex, France*

[4]*European Commission, Joint Research Centre, Institute for Transuranium Elements, Postfach 2340 D-76125 Karlsruhe, Germany*

(Received 28 May 2006; revised manuscript received 31 October 2006; published 3 January 2007)

Alloying Pu with Am stabilizes the fcc structure of δ-Pu for all temperatures and expands the lattice. δ-Pu is assumed close to the borderline of 5*f* localization. It is a nonmagnetic strongly correlated system, which should be sensitive to doping or lattice expansion. However, magnetic susceptibility, electrical resistivity, and photoelectron spectroscopy studies performed for the Pu-rich part (from 5 to 43 % Am) of the Pu-Am phase diagram indicate that the character of the 5*f* states does not vary with the Am doping. These findings are discussed within the present debate about the electronic structure of plutonium.

DOI: 10.1103/PhysRevB.75.035101 PACS number(s): 71.20.Gj, 71.27.+a, 75.30.Mb, 79.60.−i

I. INTRODUCTION

The electronic structure of pure elements is relatively well understood in the framework of the quantum theory of solids, represented by the density functional theory (DFT) and its local-density (LDA) or generalized-gradient (GGA) approximations. However, a striking exception is plutonium (Z=94). Despite its importance and the recent focused effort, the electronic structure of Pu resists a quantitative description. The main difficulty arises from the fact that the 5*f* electronic states are in a cross-over regime between localized and delocalized (itinerant) behavior. In such a situation many-body correlations in itinerant states, sometimes giving rise to qualitatively new phenomena (various exotic types of magnetic order, superconductivity, or a combination of both), can play a decisive role. The first part of the actinide series with the 5*f* states being itinerant, i.e., participating in the metallic bond, culminates with Pu. All these elements are weak paramagnets. Starting with the next element Am (Z =95), the 5*f* states are localized, nonbonding and resemble the 4*f* states in the lanthanides. They can give rise to localized 5*f* magnetism.

A certain variation of the 5*f* localization occurs already for Pu, as can be deduced from the large volume variations between Pu allotropic phases (for an overview see Ref. 1 and references therein). The volume difference between the monoclinic α-Pu phase and fcc δ-Pu, stable between 592 and 724 K, is approximately 20%. The theoretical description of this phase turns out to be the crucial issue. LDA or GGA *ab initio* calculations even in the state-of-the-art variants (see, e.g. Refs. 2–4), i.e., fully relativistic and including orbital polarization, do not reproduce the large equilibrium volume unless magnetic ordering is allowed. As experimentally no evidence for magnetic ordering exists, various other theoretical alternatives have been tested. The various theories, which predict ordered magnetism (or would do if spin polarization was permitted) at low temperature in δ-Pu, have been summarized in a recent paper, which also reviewed the experimental status.[5] Since then, muon experiments[6] have been performed and further lowered the limit for any ordered moment. Recently another variant of the LDA+U theory, called "around mean field," and based on the local spin density approximation (LSDA) succeeded to reproduce not only cohesion properties (equilibrium volume and very small equilibrium bulk modulus), but led to a principally nonmagnetic (S=0, L=0) state.[7] Qualitatively, the most advanced approaches are based on the dynamical mean field theory (DMFT), which incorporates some of the many-body interactions. Earlier work as applied to δ-Pu[8] gave a clear indication that a many-body resonance can form at the Fermi energy, E_F, even if the bare 5*f* states are clearly separated from E_F, as in the LDA+U results. In a more recent study Pourovskii *et al.*[9] have further exploited the DMFT approach and could obtain a nonmagnetic ground state for δ-Pu and also reproduce many features of the photoemission spectra, exhibiting a large peak near E_F.

Although existing experimental data leave little room for doubts with regards of the δ-Pu magnetism, it is still of a considerable interest whether δ-Pu is close to the verge of magnetism and/or localization of the 5*f* states. An interesting approach is to force a lattice expansion, which generally leads to a narrowing of electron energy bands, stabilizing eventually magnetism in spin fluctuators [e.g., 3*d* magnetism in YCo_2, due to lattice expansion obtained in the $Y(Co,Al)_2$ system[10]], or 4*f* magnetism in Ce-based valence fluctuators of Kondo systems.[11]

As is well known in the actinides, the atomic volume can serve as a very sensitive indicator of the situation of the 5*f* states. For Am (Z=95), the localization is unambiguously demonstrated by shifting the 5*f* states from the Fermi energy E_F down, to about 2 eV binding energy, as indicated by the photoelectron spectroscopy.[12] Comparing the atomic volume of Pu and Am, we observe that δ-Pu is about half-way between α-Pu and Am. The large atomic volume of Am collapses rather easily under pressure, and from 17 GPa to at least 100 GPa forms an orthorhombic crystal structure, the

symmetry of which reflects the 5*f* involvement in metallic bonding.[13] The Am ground-state structure at ambient pressure is double hexagonal close packed (dhcp), but it transforms to a fcc structure at the pressure $p=6.1$ GPa.[13] The lattice parameter at 6.5 GPa is 461.3 pm. This fcc structure is not only identical to the high-temperature phase observed for Am above 650 °C, but also to the structure of δ-Pu. Thus an extended range of the fcc structure exists in the Pu-Am phase diagram, which shrinks somewhat from a nearly complete miscibility at high temperatures to the range characterized as 5%–75% Am content in the low-T limit. As the lattice parameter expands considerably with increasing Am concentration, the system offers a unique possibility to study the effect of lattice expansion on Pu. On the other hand, the effect of lattice compression on Am can be only relatively small, as the compression does not reach values obtained in high-pressure experiments.

This article aims to cover basic characterization of the fcc Pu-Am system, ranging from 5 to 43 % doping of Pu with Am. An x-ray diffraction study was followed by using bulk experimental methods (magnetic susceptibility, electrical resistivity), and the study was complemented by photoelectron spectroscopy, consisting of core-level x-ray photoelectron spectroscopy (XPS) and high-resolution ultraviolet photoelectron spectroscopy. This work represents also a continuation of the effort to map the behavior of δ-Pu stabilized by one or more dopants.[14]

II. EXPERIMENTAL DETAILS

A. Samples

The Pu-Am alloys were synthesized at the Institute for Transuranium Elements (ITU). The samples (300–400 mg for each alloy) were prepared by arc melting of 2N purity ^{239}Pu (half-life 24 000 years) and ^{241}Am (half-life 432 years) metals in stoichiometric amounts and casting into copper molds. As cast samples were analyzed by x-ray diffraction (XRD) at ITU. Each sample was cut into two pieces, one was used for UPS/XPS measurements, while all other studies were performed on the other piece (mass of about 300 mg). In particular, we first performed magnetic susceptibility measurements. After that, it was laminated to a thickness of about 200 μm and annealed for 3 h at 450 °C under high vacuum in order to remove defects imposed by the lamination and self-irradiation defects (vacancies and interstitials) created by α decays. As a next step, XRD at CEA and electrical resistivity measurements were performed.

Due to the low amount of alloy available, a standard chemical analysis could not be performed. Only α spectroscopy and electron probe microanalysis (EPMA) measurements were undertaken to quantify the ^{241}Am content. Results are displayed in Table I and given in atomic percent, which are used also in the text. Optical microscopy and x-ray mapping obtained by EPMA proved that all alloys were single phase.

B. Experimental setup

X-ray diffraction experiments were performed using a classical θ-2θ diffractometer (Siemens D500) with a Cu-K_α radiation, secondary graphite monochromator, and scintillation detector. The obtained lattice parameters are listed in Table I.

TABLE I. Comparison of the composition of the samples studied obtained by different methods and its lattice parameter.

Am nominal composition (at. %)	Am concentration α-spectroscopy (at. %)	Am concentration EPMA (at. %)	a (pm) ±0.05
24	24±0.2	23.5±0.5	472.53
20	22.5±0.2	18.0±2	470.09
15	15±0.2	13.6±0.5	469.21
8	7.9±0.2	7.5±0.5	467.65
5	4.9±0.2	4±0.5	465.14

Magnetic measurements were performed using two devices, a Manics Faraday balance susceptometer (at CEA) and a Quantum Design SQUID magnetometer (at ITU). For the Faraday balance technique, a sample of a mass of about 300 mg was first sealed in a quartz tube (under He atmosphere), then placed in gold cylinders (to reduce the magnetic response from the sample holder), and finally enclosed in aluminum containers (under helium atmosphere). Temperature was measured by means of a Rh/Fe sensor located at the bottom of the cryostat. For the SQUID, the mass of the sample was between 10 and 200 mg, depending on the alloy; the sample was confined in a Plexiglas tube placed in a nickel-silver ($Cu_{62}Ni_{18}Zn_{20}$) container, both sealed under helium gas. For each sample, a complete reference sample holder was measured in the entire temperature range before loading the sample. Although its length exceeds the distance between the SQUID pick-up coils and its movement should not affect the SQUID signal in a first approximation, there is still the effect of a moving cavity in a diamagnetic material, so the sample holder signal is effectively paramagnetic, and for small samples (10 mg) it represents about half of the total signal with the sample mounted, which reduces the absolute accuracy. Moreover, this method cannot discern possible effects of α particles on the Plexiglas, which becomes even visually stained for higher Am concentrations after several months.

Electrical resistivity was measured by a standard four-probe method.

Photoelectron spectroscopy experiments were performed at ITU Karlsruhe by means of a spectrometer equipped with Leybold LHS 10 hemispherical analyzer, which is placed in a glove box. X-ray photoelectron spectra (XPS) were taken using the Al-K_α radiation (1486.6 eV). It was not monochromatized, but the satellite was removed by a numerical procedure. The energy resolution (combined line width and instrumental resolution) is about 1.0 eV. Ultraviolet photoelectron spectroscopy (UPS) was studied using the HeI (21.22 eV) and HeII (40.81 eV) excitation radiation. Exact binding energies were calibrated with a precision better than 0.01 eV using the Au Fermi edge.

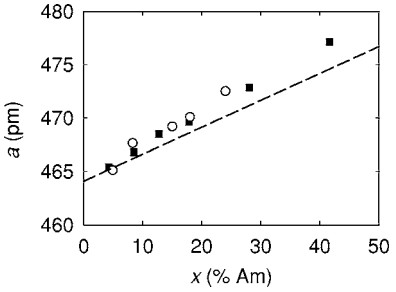

FIG. 1. Variations of the lattice parameter a of $Pu_{1-x}Am_x$ solid solutions for different Am concentrations. Our data (empty circles) are compared with those in Ref. 15 (full squares). The dashed line represents the interpolation between the values estimated for pure Pu and Am, derived as described in the text.

III. RESULTS

A. X-ray diffraction

All XRD spectra exhibit sharp lines of the fcc structure. The lattice parameter a (listed in Table I) of the binary alloys increases gradually with increasing Am concentration (Fig. 1), as expected on the basis of earlier studies.[15] The dashed line represents a linear interpolation between pure δ-plutonium (face centered cubic with a=464.1 pm) and pure β-americium (face centered cubic with a=489.3 pm), obtained by extrapolation from their respective high-temperature ranges of stability.

It is interesting to note that already the sample with lowest Am concentration (detailed analysis shows 4.9 at. % Am) is fully in the fcc range, i.e., no martensitic transformation happens even when cooled to low temperatures. In this respect, the Am stabilization of the fcc phase is more efficient than, e.g., Ce.[14]

B. Magnetic susceptibility

Magnetic susceptibility $\chi(t)$ of Pu can be characterized as relatively low and only weakly temperature dependent. This is true not only for the α phase ($\chi \approx 0.66 \times 10^{-8}$ m^3/mol, but also for the least delocalized δ phase, for which an even lower value $\chi \approx 0.64 \times 10^{-8}$ m^3/mol, was reported.[16] Apparently the highest value and some temperature dependence was observed in the narrow temperature range of existence recorded for β-Pu ($\approx 0.69 \times 10^{-8}$ m^3/mol).[16]

Although Am does not form local magnetic moments, its susceptibility is higher. There is variation between values found by different authors, undoubtedly as a consequence of the difficulty of purification. They scale from 0.85×10^{-8} m^3/mol (Ref. 17) to 1.10×10^{-8} m^3/mol (Ref. 18 and one of the samples studied in Ref. 19). The higher susceptibility of Am comparing to Pu was attributed not to an enhanced density of states at the Fermi level (which is actually much smaller) but to the Van Vleck susceptibility of the $5f^6$ ionic state, which although nonmagnetic (J=0), has a low-lying excited magnetic state. Such a susceptibility is essentially independent of temperature. The weak low-temperature upturn observed, which has an approximate Curie form, could be due to a small amount of impurity atoms with magnetic moments.

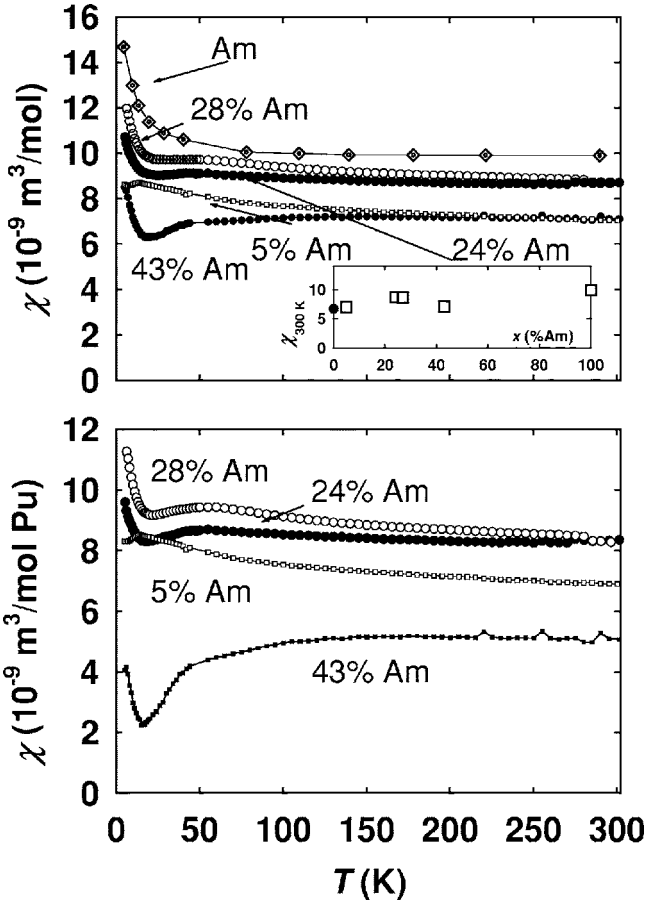

FIG. 2. Temperature dependence of magnetic susceptibility $\chi(T)$ of $Pu_{1-x}Am_x$ alloys for selected Am concentrations, obtained using the SQUID magnetometer. In the upper part, molar susceptibilies are displayed, while identical data are redrawn after subtraction of Am susceptibility in the lower part. The inset illustrates the weak temperature dependence of magnetic susceptibility at T=300 K as a function of Am concentration. Pure Am data are taken from Ref. 19 and the dot for x=0 is taken from the high-temperature susceptibility measurement of δ-Pu in undoped form and corresponds to T =600 K (Ref. 16).

For further analysis we take as the most plausible the value reported for the Am sample, studied by Kanellakopulos *et al.*[19] on a sensitive Faraday balance magnetometer. This data set is included in Fig. 2, in which we show the values for the alloys as well as an attempt to estimate the contribution from Pu only (lower part of Fig. 2). Our analysis shows that these data can be tentatively described as a sum of a temperature-invariant term 0.96×10^{-8} m^3/mol, and a Curie term C/T, where C is the Curie constant. The Curie term and the low value of the effective moment per Am atom, μ_{eff} =0.16 μ_B, suggest that noninteracting impurity magnetic moments may be responsible for the whole temperature dependence. If assuming ionic effective moments of Np ($5f^4$), 2.68 μ_B, we obtain about 0.3–0.4 at. % Np. The article[19] admitted the presence of 0.1% Np, coming from decay processes. For example, ^{241}Am can produce about 0.2% ^{237}Np during approximately one year. However, any other magnetic impurities (e.g., transition metals) can have a similar impact.

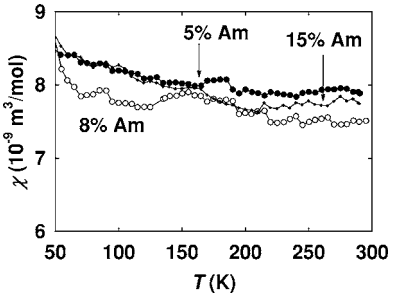

FIG. 3. Temperature dependence of magnetic susceptibility $\chi(T)$ of $Pu_{1-x}Am_x$ alloys for selected Am concentrations, obtained using the Faraday balance method.

So as to estimate the susceptibility variations of the Pu subsystem, we may tentatively assume that the Van Vleck susceptibility of Am, which is a single-ion property, does not change much if surrounded by Pu. The supporting argument is the invariable character of Am XPS spectra, which do not indicate any sign of delocalization of Am-5*f* states in Pu-Am, at least over the doping range examined in this study. We also assume that the susceptibility value found in dhcp Am represents that also in the fcc phase. As the impurity contents of Am were not known, we considered the presence of the impurity Curie term as in Ref. 19. The experimental uncertainty in the susceptibility of Am naturally affects, in particular for a higher Am content, the susceptibility deduced for Pu in Am. The values of total magnetic susceptibility for all studied Am concentrations up to 43% were found low, in the 10^{-9} m^3/mol range, and weakly concentration dependent, without any anomaly pointing to a magnetic ordering.

The weakly temperature dependent character of the susceptibility is seen in Fig. 2, summarizing data obtained from the SQUID magnetometer. These data (based on measurements in 5 and 7 T) are more precise than the Faraday balance data. On the other hand, the Faraday balance measurement (Fig. 3) is more direct than for the SQUID, which makes the sample container correction more transparent, and we include the Faraday balance data for confirmation.

All samples except the highest Am concentration studied (43% Am) exhibit a weakly increasing susceptibility χ with decreasing T in the high-temperature range. Such dependence can be formally described by a modified Curie-Weiss law $\chi=\chi_0+C/(T-\theta_p)$, but the temperature-independent term χ_0 accounts for the major part of total susceptibility and the paramagnetic Curie temperature θ_p comes out large ($|\theta_p| > 400$ K) and negative even for the apparently most temperature-dependent sample (5% Am), which makes the interpretation in terms of local magnetic moments implausible. At lower temperatures $\chi(T)$ forms a plateau and a low temperature tail, approximately Curie-like (see Fig. 2), almost certainly indicating the presence of magnetic impurities. Although part of the tail can be related to the Am content, recent Pu aging experiments[20] show that radiation damage induces such Curie tail also in Pu metal. In addition, also, effects of radiation damage of the sample holder (capsule) must be considered, especially for higher Am content. However, a detailed examination of aging effect has not been addressed in this work.

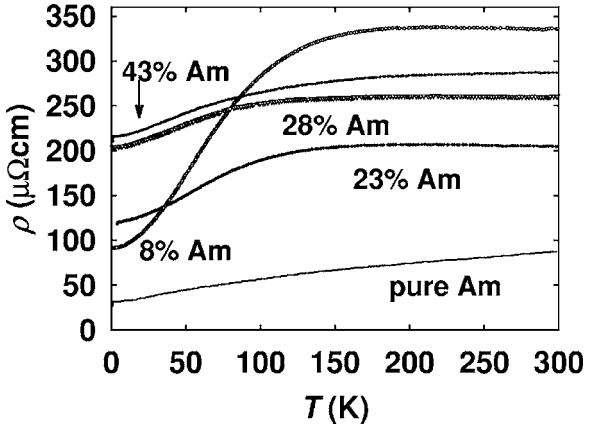

FIG. 4. Temperature dependence of electrical resistivity of $Pu_{1-x}Am_x$ alloys for selected Am concentrations. Pure Am curve is taken from Ref. 23.

Such types of temperature dependence of magnetic susceptibility are reminiscent of one class of spin fluctuators, with a characteristic temperature of spin fluctuations related to the beginning of a plateau in $\chi(T)$, which follows the high-temperature part resembling a Curie-Weiss term. Typical representatives are UAl_2 (Ref. 21) or URuGa (Ref. 22), but both exhibit susceptibility an order of magnitude higher than the Pu-Am alloys. In addition, for the Pu-Am alloys only a small fraction of the total susceptibility conforms to the spin-fluctuation scheme. The similarity can be also extended to electrical resistivity (discussed in the next section).

A somewhat different character was found for the sample with the highest Am concentration studied. In this case, χ is lower and tends to decrease with decreasing T, but the low-T tail appears in analogy with other samples. Lower values are particularly striking when evaluated per Pu atom. Because this sample was very small and corrections for the sample holder consequently quite severe, the tendency of decreasing susceptibility with increasing Am concentration has still to be confirmed and extended to even higher Am content. The main conclusion from the susceptibility results is that neither total susceptibilities, nor the deduced Pu contribution, increase with Am doping.

C. Electrical resistivity

The temperature dependences of electrical resistivity were studied on the samples prepared from the same batches as those used for susceptibility measurements. On the timescale of the experiment an increase of resistivity due to the self-irradiation damage can be observed, but remains relatively weak (below 1 $\mu\Omega$ cm). The low-temperature behavior below about 30 K, which is analyzed here in more detail, is affected in an additive way, which does not deform the type of the temperature dependence. The results, together with earlier results obtained by Gomez-Marin[23] are displayed in Fig. 4.

In general, all $\rho(T)$ curves have the type of dependence observed previously for δ-Pu stabilized by various dopants to low temperatures, i.e., with a broad knee around 150 K and a

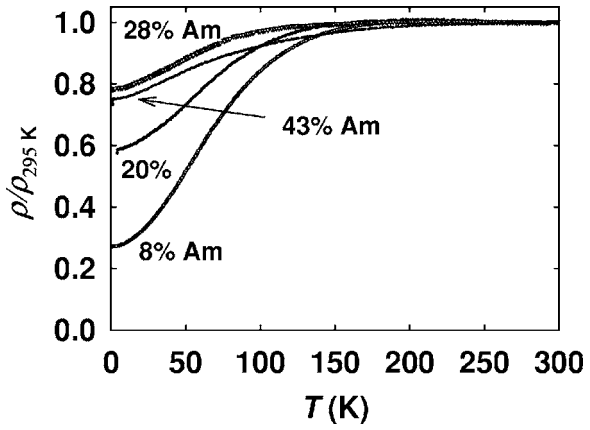

FIG. 5. Resistivity of selected $Pu_{1-x}Am_x$ alloys normalized to resistivity values at $T=295$ K.

saturation at high temperatures.[24] This resistivity type is actually less anomalous than for α-Pu, in which the knee is located at lower temperatures (80 K), more pronounced, and even forming a maximum for some current direction.[25] The fact that the room-temperature resistivity varies in a somewhat nonsystematic way is probably due to a large uncertainty introduced by the geometrical factor. Apart from those absolute values, the resistivities can be seen as regular. For δ-Pu with low doping level, resistivities (at room temperature) as low as 110 $\mu\Omega$ cm have been recorded,[24] and the same dependence of $\rho(T)$ was found for different levels of δ-stabilizing dopings,[14] with absolute values increased for higher doping due to the impurity scattering, so that the Matthiessen's rule seems to be obeyed.

The effect of geometrical factor is eliminated in Fig. 5, which displays resistivities normalized to the room-temperature value, making more apparent the expected gradual increase of residual resistivity with increasing Am concentration for samples up to 28% Am. For 43% Am, the character is somewhat different, the saturation at high T is slower, and the residual resistivity ratio ($\rho_0/\rho_{300\ \mathrm{K}}$) even slightly lower than for 28% Am. The subtle, but qualitative change is more apparent from Fig. 6, which displays concentration dependencies of relative resistivities for all samples.

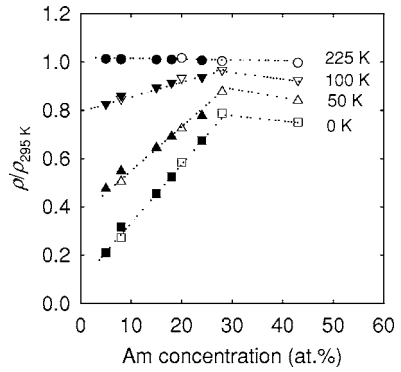

FIG. 6. Isotherms of relative electrical resistivity at $T=0$, 50, 100, and 225 K. Full symbols: this work; open symbols: Ref. 22. The data at $T=0$ K were obtained by extrapolation using the $\rho=aT^2$ relation.

As only the Pu sublattice can bring a high density of quasiparticle states to the Fermi level, the changes are understandable. The disorder scattering in the Pu-Am system does not lead to such a dramatic increase or residual resistivity ρ_0 as, for example, in the Pu-Np system,[26] in which both components contribute to the states at E_F. In the Pu-Am system, the active sublattice simply becomes diluted. The knee around 150 K and the high-temperature saturation of $\rho(T)$ cannot be associated with any particular model, as different kinds of instability of localized states or local magnetic moments (spin fluctuations, Kondo, valence fluctuations) lead to a qualitatively similar behavior.[27,28] The high-temperature resistivity study shows that $\rho(T)$ resumes a weakly increasing tendency, similar for all Am concentrations studied, between 500 K and 700 K.[23] This increase can be attributed to electron-phonon scattering, which becomes more apparent when other scattering mechanisms saturate.

The analysis of the low-T part shows that $\rho(T)$ scales as T^2 for all the samples up to about 40 K. Only in one case (8% Am, $a=0.036$ $\mu\Omega$ cm K^{-2}) does the value of the prefactor a exceed that recorded for α-Pu (0.021 $\mu\Omega$ cm K^{-2} in Ref. 25). If we neglect the relatively large inaccuracy due to the geometrical factor uncertainty, we could calculate tentatively the coefficient of the low-temperature specific heat $\gamma=60$ mJ/mol K^2 for $Pu_{0.92}Am_{0.08}$ by using the Kadowaki-Woods relation[29] $a/\gamma^2=10^{-5}$ (in the units $\mu\Omega$ cm K^{-2} and mJ/mol K^2, respectively). This is in good agreement with γ estimated for Al-doped δ-Pu (64 mJ/mol K^2 in Ref. 30) and somewhat higher than estimated for $Pu_{0.92}Am_{0.08}$. (35–55 mJ/mol K^2).[31] The same method applied on other samples would yield $\gamma=37-41$ mJ/mol f.u. K^2 for the samples up to 43% Am, which corroborates, as indicated,[31] the lack of any increase of γ. The γ values would be higher if expressed per mole of Pu, as the γ value of Am itself is substantially lower (2 mJ/mol K^2 in Ref. 32). Such procedures have to be taken with caution, as, for example, the Am resistivity data shown in Fig. 4 yield $a=0.0068$ $\mu\Omega$ cm K^{-2}, corresponding thus to a much higher γ (26 mJ/mol K^2). The main message, however, is clear—γ values, as deduced from resistivity, in the Pu-Am system do not increase above the δ-Pu value. It would be interesting to study the variations of γ directly for higher Am concentrations.

D. photoelectron spectroscopy

To investigate possible further localization by a local-probe technique, we performed a photoelectron spectroscopy study of several Pu-Am alloys, prepared *in situ* by the same method of thin-layer synthesis, as used before for pure Pu.[33] Typical thickness of the layers exceeded 10 nm, i.e., it was larger than the information depths of photoelectron spectroscopies. Si wafers or polycrystalline Mg were used as a substrate. We used two different Pu-Am alloy targets containing 15 and 25 % Am, respectively. The primary check of the deposited material was done by x-ray photoelectron spectroscopy (XPS). The energy scale was calibrated using the Fermi level of Au. The spectra indicated that only Pu and Am were present. The Am/Pu ratio determined directly in the

XPS information depth by comparison of the intensities of Pu and Am 4*f*-core level lines showed that it differed somewhat from the target composition. We attributed this to a segregation of Am in the surface and subsurface area of the target, depending on its temperature variations, and it allowed us to prepare layers with a broader composition range than covered by the initial composition of the targets.

Some features of Pu spectra are very sensitive to oxygen contamination.[34] Therefore we monitored in all cases the O -2*p* line in UPS spectra. This line appearing at 5–6 eV binding energy (BE) is a more sensitive indicator of the sample quality than the O-1*s* seen in XPS, and its absence means that our layers are as oxygen free as the best Pu surfaces in Ref. 33. Important spectroscopic information on the degree of 5*f*-delocalization can be obtained from the actinide 4*f* spectra. In the itinerant case, the 5*f* states can redistribute immediately due to the Coulomb screening around the 4*f* hole left after the photoexcitation process, thus reducing the final-state energy E_f. The kinetic energy of the photoelectron is consequently higher. In the case of localized 5*f* states, the valence-band *s*, *p*, and 6*d* conduction electrons are responsible for the screening. E_f is higher, because those states are more separated (in real space) from the 4*f* states than the 5*f* states. The photoelectron kinetic energy is therefore lower and they appear at higher binding energy. The convention is to denote the feature due to the 5*f* screening as "well screened," whereas the ones coming from the non-*f* screening are denoted as "poorly screened."[35] We have shown that the broad and approximately symmetric "poorly screened" peaks dominate the 4*f* spectra in Pu systems with localized 5*f* states [e.g., PuSb (Ref. 36)]. In α- and δ-Pu, the narrow asymmetric well-screened features at 2.3 eV lower BE (its higher intensity in α- comparing to δ-Pu can be even better assessed from high-resolution data obtained in a synchrotron experiment)[37] can contain about half of the total spectral intensity.[33] This two-channel screening model not only explains essential features seen in the core-level spectra, but it qualitatively corresponds to more sophisticated quantitative analyses of spectra when crossing the Mott-Hubbard transition (see, e.g., Ref. 38.) The spin-orbit split Am $4f_{5/2}$ and $4f_{7/2}$ core-level spectra of Am (not shown here) are symmetric, located at respective binding energies 463.1 eV and 448.9 eV (the binding energies are related to the Fermi level), which corresponds to literature data for Am metal.[12] For higher Am concentrations one can even distinguish weak satellites at lower BE, separated from the main lines by 3.8 eV. The satellites are taken as residual well-screened peaks, i.e., fingerprints of a very weak hybridization of the Am-5*f* states.[12] We can conclude that Am-5*f* states have nearly pure atomic character. We know from the high-pressure studies of Am (Ref. 13 and 39) that the compression to a relative volume of ≈80% is necessary to produce AmIII and the start of the delocalization. In our studies even at the δ-Pu volume the compression of Am is only equivalent to 91% of its ambient value, so we would certainly not expect the Am 5*f* states to become delocalized.

The two Pu-4*f* peaks exhibit both well-screened and poorly screened features. Investigation of $Pu_{1-x}Am_x$ layers with x=0.20, 0.22, 0.26, 0.28, and 0.33 shows that the exact Am content does not affect the shape, reflecting that the proportions of well- and poorly screened features do not vary in this concentration range. The inspection of the Pu-4*f* spectra shown in Fig. 7, in particular the height of the well-screened $4f_{7/2}$ feature, which is better resolved than for the $4f_{5/2}$ one, points to the same character as in δ-Pu, and we therefore conclude that the 5*f* delocalization is not affected by the Am doping and related volume expansion. We can see that the narrow well-screened line is somewhat reduced in δ-Pu (*b*) comparing to α-Pu (*a*), but it stays on the δ-Pu level with the Am doping. The spectrum (*c*) obtained for $Pu_{0.74}Am_{0.26}$ can be taken as a representative of all layers with Am concentration x up to 0.33. A difference with respect to the spectrum (*b*) is negligible.

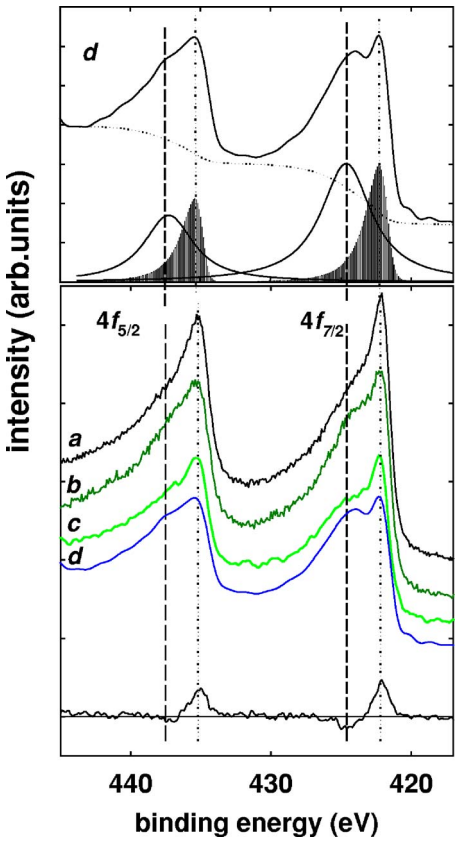

FIG. 7. (Color online) Detail of Pu-4*f* spectra. *a*—Pu layer deposited at T=77 K represents α-Pu. *b*—spectrum representing δ -Pu on Pu surface subjected to annealing (see Ref. 33). The difference (displayed at the bottom) between *a* and *b* helps to visualize that the well-screened features (marked by dotted lines) are somewhat suppressed in δ-Pu relatively to the poorly screened ones (marked by dashed lines). The spectrum *c* of $Pu_{0.74}Am_{0.26}$, has the character similar to the spectrum *b*. The spectra vary somewhat only for *d* $Pu_{0.64}Am_{0.36}$, which was the highest Am concentration with 4*f* spectra studied.The upper panel shows the decomposition of the spectrum *d* into the well-screened and poorly screened components.

Small changes were observed only for higher Am concentrations. Around $Pu_{0.64}Am_{0.36}$ we found the well-screened feature reduced compared to the poorly screened one, which may be interpreted as a somewhat higher degree of localization of the 5*f* states. It concerns layers with x=0.36 (spectrum *d*) and 0.37. Compared with the dramatic variations

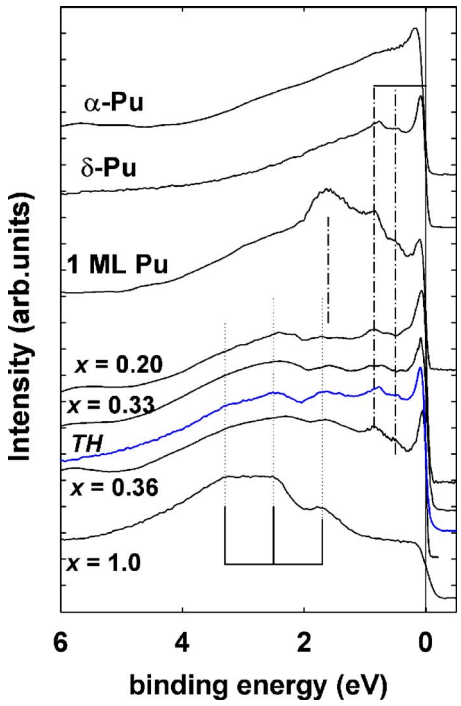

FIG. 8. (Color online) UPS spectra with the HeII photoexcitation (40.81 eV). The spectra of the $Pu_{1-x}Am_x$ layers are marked by the respective x values. The full lines mark the position of the 5*f* features in pure Am (at the bottom, taken from Ref. 12). The dash-dotted lines mark the positions of Pu-related lines. At the top, spectra of bulk α- and δ-Pu (the latter from Ref. 41) are shown for comparison, as well as the spectrum of one monolayer of Pu on Mg. The spectrum labeled TH is "theoretical" spectrum obtained by superposition of weighted (corresponding to the concentration of 33% Am) spectra of pure δ-Pu and Am.

observed in ultrathin layers,[33] the changes here are modest and remain to be investigated for even higher Am concentrations.

Although a precise quantification of the spectral intensity in the well- and poorly screened peaks is difficult, we tried to make a similar decomposition of the peaks as in Ref. 33, assuming the Voigt shape (convoluted Lorentzian and Gaussian) for the poorly screened peaks, and asymmetric Γ functions for the well-screened peaks. In this way we obtain up to 0.50 of the spectral intensity in the well-screened peaks for pure Pu, whereas this amount is reduced below 0.10 of the total intensity in one Pu monolayer on Mg.[33] For the high Am concentrations we obtained about 27% of the spectral intensity in the well-screened peaks. This is consistent with the fact that the 4*f* spectra of $Pu_{0.64}Am_{0.36}$ would fit between those obtained on 3 and 5 ML of pure Pu on Mg, i.e., into a presumably intermediate 5*f* localization situation.[33]

UPS valence-band spectra recorded with a typical energy resolution of 45 meV can be seen in Fig. 8. The HeII spectra ($h\nu$=40.81 eV) reflect mainly the photoemission from the 5*f* states. Pure Am (at the bottom) has the 5*f* states several eV below E_F, and the spectra exhibit a final state multiplet, reached from the $5f^6$ ground-state configuration. The typical featureless triangular spectrum of α-Pu (Ref. 33) is at the top. The difference with respect to α-Pu spectra in Ref. 40, which exhibits clear features of δ-Pu, was explained[33] by the surface treatment leaving the δ-Pu character of structure at the surface in the latter case. The real δ-Pu spectrum (Pu with few percent Al) shown below exhibits another maximum at 0.85 eV BE, and a weak feature at about 0.5 eV. The spectra of $Pu_{1-x}Am_x$ for x=0.20–0.33 are all very similar to each other. They clearly reflect the features seen for pure Am.[12] We cannot unambiguously identify the feature at 1.7 eV, which occurs in Am, but 5*f*-intensity appears in this energy range also when the Pu 5*f* states localize in ultrathin layers. To assess individual contributions of Pu and Am, we constructed a "theoretical" Pu-Am spectrum consisting of 35% of Am and 65% of δ-Pu spectra, which were normalized (after subtracting the secondary electron background) to the same total intensity. The Am spectrum was also multiplied by 6/5 because of assumed different 5*f* electron count in Pu (5) and Am (6). The result denoted as *TH* is practically identical with all Pu-Am spectra in this concentration range. This means that whatever phenomena are reflected in the δ-Pu spectra, they remain essentially unchanged if doped with Am, and the emission at 1.7 eV is only due to Am. Similar as in the 4*f* spectra, the shape of the valence-band spectra varies for x=0.36. It may be understood as a small step toward the 5*f* localization in Pu, which would reduce the 5*f* signal in the vicinity of E_F.

IV. DISCUSSION AND CONCLUSIONS

Bulk properties, namely magnetic susceptibility and electrical resistivity, do not show clear anomalies or abrupt variations with addition of Am. Such changes would indicate the onset of magnetic ordering or the Pu-5*f* localization, which is predicted by most band theories for a lattice expansion ($\Delta V/V \approx 8\%$ for 40% Am). In the Pu-rich part of the Pu-Am phase diagram, magnetic susceptibility retains its relatively low value and weak temperature dependence. The electrical resistivity also maintains the characteristics observed for δ-Pu, with a broad knee and a tendency to saturation. Some features in susceptibility and resistivity are reminiscent of spin fluctuators with high spin-fluctuation energy, but doping with Am does not lead to an apparent change of any spin fluctuations. In fact α-Pu and especially β-Pu resitivities with a low-T maximum and pronounced negative slope, $d\rho/dT<0$, have clearly stronger features of a characteristic low energy scale (low characteristic spin-fluctuation temperatures) than δ-Pu.[42]

As a main conclusion from the photoelectron spectroscopy data we showed that the characteristics of the 5*f* states remain preserved, despite the volume expansion, in Am-doped δ-Pu, although the situation may somewhat change for Am concentrations over about 30%. One should bear in mind that the concentrations determined by means of XPS can be affected by systematic errors in integrating the partly overlapping Pu and Am peaks. As the present study concentrated on the Pu-rich part of the Pu-Am alloys, it is still to be seen whether this character is preserved in the Am-rich part.

How can these conclusions be understood? It is very likely, and it is also shown by photoelectron spectroscopies, that δ-Pu is somewhat more localized than α-Pu. At present

the electronic configuration of Pu is under considerable debate. As stated in the Introduction, most band-structure calculations obtain a configuration close to $5f^5$ and, at the same time, predict magnetic ordering. The latter does not occur,[5] however, x-ray absorption and electron-energy loss spectroscopy (EELS) point to a configuration close to $5f^5$.[43] On the other hand, EELS measurements for the oxides (Ref. 44, Fig. 2) report a configuration for UO_2 of $5f^3$ and for PuO_2 as $5f^5$, which is in disagreement with the accepted configurations of $5f^2$ and $5f^4$ for UO_2 and PuO_2, respectively.[45] Thus, the establishment of the exact electron count for metallic Pu appears difficult and we note that in the Pu chalcogenides, which display no magnetic ordering and almost temperature-independent susceptibility, the electron count has been proposed substantially above $5f^5$ (Refs. 46–48), as well as an older work proposing intermediate valency in PuTe (Ref. 49). Thus, the idea that there are *more* than five electrons in the $5f$ electronic state of Pu and its compounds is not new.

Recently, varieties of LDA+U or LSDA+U methods yield the $5f$ count close to 5.5 without artificially forcing any part of the f states into localization.[7,9,50] These theories suggest the occupancy of the electronic ground state has about 5.5 $5f$ electrons, with about 0.5 of a hole in the $5f_{5/2}$ subband existing due to the hybridization with non-f states. Such ground state has then no magnetic moment ($S_z=0$, $L_z=0$). Although such situation still remains to be confirmed by experimental techniques,[51] the Pu-Am data presented in this article may be interpreted within this model. The LDA+U calculations in Ref. 7 suggest that the $5f$ states are in δ-Pu largely shifted from E_F already, although still forming a narrow band of one-electron states, with the main part about 1 eV broad. Such situation is not critically sensitive to any volume expansion, as the ground state stays nonmagnetic. Many-body correlations or intramultiplet excitations can be then responsible for the quasiparticle states at E_F.[9] The LDA+U calculations, recently extended to Am and Pu-Am alloys,[52] corroborate this picture. For pure Am, they correctly reproduce the nonmagnetic $5f^6$ state, which remains stable in the course of dilution with Pu, remaining below the lower edge of the conduction band. Also the Pu-$5f$ states are little affected by the alloying with Am as well as by the lattice expansion. Such a model also explains the weak concentration dependence of the γ coefficient of Pu with Am doping.[31]

In general, we can conclude that Am doping in δ-Pu does not, despite the large volume expansion by 8%, lead to magnetism or any dramatic localization of the Pu-$5f$ states. Such situation can be tentatively attributed to the fact that δ-Pu has a complex electronic ground state with an electron count greater than $5f^5$, whereas Am has a well-defined $5f^6$ configuration. This contradicts expectations based on $5f$ band (LDA or GGA) theories. The particular case of $Pu_{0.75}Am_{0.25}$ was calculated in Ref. 53, concluding a dramatic variation compared to δ-Pu especially close to E_F, which is in disagreement with our data. Our results are therefore supportive for description of δ-Pu in terms of LDA+U or DMFT theories, for which the results on δ-Pu are likely to be much less sensitive to an expansion.

ACKNOWLEDGMENTS

The authors appreciate fruitful discussions with M. J. Fluss and A. B. Shick and are grateful to D. Bouëxière for technical support in the samples characterization. The work of L.H., supported by the Grant Agency of the Czech Republic under Grant No. 202/04/1103, is also a part of the research program MSM 0021620834 financed by the Ministry of Education of the Czech Republic.

[1] S. S. Hecker, D. R. Harbur, and T. G. Zocco, Prog. Mater. Sci. **49**, 429 (2004).
[2] P. Söderlind and B. Sadigh, Phys. Rev. Lett. **92**, 185702 (2004).
[3] P. Söderlind, Europhys. Lett. **55**, 525 (2001).
[4] P. Söderlind, A. Landa, and B. Sadigh, Phys. Rev. B **66**, 205109 (2002).
[5] J. C. Lashley, A. Lawson, R. J. McQueeney, and G. H. Lander, Phys. Rev. B **72**, 054416 (2005), and references therein.
[6] R. H. Heffner, G. D. Morris, M. J. Fluss, B. Chung, S. McCall, D. E. MacLaughlin, L. Shu, K. Okishi, E. D. Bauer, J. L. Sarrao, W. Higemoto, and T. U. Ito, Phys. Rev. B **73**, 094453 (2006).
[7] A. B. Shick, V. Drchal, and L. Havela, Europhys. Lett. **69**, 588 (2005).
[8] S. Y. Savrasov, G. Kotliar, and E. Abrahams, Nature (London) **410**, 793 (2001).
[9] L. V. Pourovskii, M. I. Katsnelson, A. I. Lichtenstein, L. Havela, T. Gouder, F. Wastin, A. B. Shick, V. Drchal, and G. H. Lander, Europhys. Lett. **74**, 479 (2006).
[10] T. Goto and M. I. Bartashevich, J. Phys.: Condens. Matter **19**, 3625 (1992).
[11] J. G. Sereni, J. Alloys Compd. **207/208**, 229 (1994).
[12] J. R. Naegele, L. Manes, J. C. Spirlet, and W. Müller, Phys. Rev. Lett. **52**, 1834 (1984); J. R. Naegele, J. Ghijsen, and L. Manes, in *Actinides—Chemistry and Physical Properties, Structure and Bonding* 59/60 (Springer-Verlag, Berlin-Heidelberg, 1985), pp. 197–262.
[13] A. Lindbaum, S. Heathman, K. Litfin, Y. Meresse, R. G. Haire, T. Le Bihan, and H. Libotte, Phys. Rev. B **63**, 214101 (2001).
[14] M. Dormeval, N. Baclet, C. Valot, R. Rofidal, and J. M. Fournier, J. Alloys Compd. **350**, 86 (2003).
[15] F. H. Ellinger, K. A. Johnson, and V. O. Struebing, J. Nucl. Mater. **20**, 83 (1966).
[16] C. E. Olsen, A. L. Comstock, and T. A. Sandenaw, J. Nucl. Mater. **195**, 312 (1992).
[17] M. B. Brodsky, in AIP Conf. Proc. No. 5, *Magnetism and Magnetic Materials—1971*, edited by C. D. Graham, Jr. and J. J. Rhyne, (AIP, New York 1972) pp. 611–629.
[18] D. B. McWhan, thesis, University of California UCRL-9695, 1961.
[19] B. Kanellakopulos, A. Blaise, and J. M. Fournier, Solid State Commun. **17**, 713 (1975).
[20] S. McCall, M. J. Fluss, B. Chung, G. Chapline, M. McEllfresh, D. Jackson, N. Baclet, L. Jolly, and M. Dormeval, in *Recent Advances in Actinide Science*, edited by I. May, R. Alvares, and N.

Bryan (RSC, Cambridge, 2006), pp. 734–736.
[21] V. Sechovský and L. Havela, in *Ferromagnetic Materials—A Handbook on the Properties of Magnetically Ordered Substances*, edited by E. P. Wohlfarth and K. H. J. Buschow (North-Holland, Amsterdam, 1988), Vol. 4, pp. 309–491, and references therein.
[22] V. Sechovský and L. Havela, in *Handbook of Magnetic Materials*, edited by K. H. J. Buschow (North-Holland, Amsterdam, 1998), Vol. 11, pp. 1–289, and references therein.
[23] E. Gomez-Marin, Ph.D. thesis, University of Joseph Fourier, Grenoble, 1992.
[24] M. B. Brodsky, Phys. Rev. **163**, 484 (1967).
[25] A. J. Arko, M. B. Brodsky, and W. J. Nellis, Phys. Rev. B **5**, 4564 (1972).
[26] C. E. Olsen and R. O. Elliott, Phys. Rev.. **139**, A437 (1965).
[27] M. B. Brodsky, Phys. Rev. B **9**, 1381 (1974).
[28] A. Freimuth, J. Magn. Magn. Mater. **68**, 28 (1987).
[29] K. Kadowaki and S. B. Woods, Solid State Commun. **58**, 507 (1986).
[30] J. C. Lashley, J. Singleton, A. Migliori, J. B. Betts, R. A. Fisher, J. L. Smith, and R. J. McQueeney, Phys. Rev. Lett. **91**, 205901 (2003).
[31] P. Javorsky, L. Havela, F. Wastin, E. Colineau, and D. Bouëxière, Phys. Rev. Lett. **96**, 156404 (2006).
[32] J. L. Smith, G. R. Stewart, C. Y. Huang, and R. G. Haire, J. Phys. (France) **40**, C4-138 (1979).
[33] L. Havela, T. Gouder, F. Wastin, and J. Rebizant, Phys. Rev. B **65**, 235118 (2002).
[34] M. T. Butterfield, T. Durakiewicz, E. Guziewicz, J. J. Joyce, A. J. Arko, K. S. Graham, D. P. Moore, and L. A. Morales, Surf. Sci. **571**, 74 (2004).
[35] J. C. Fuggle, M. Campagna, Z. Zolnierek, R. Lässer, and A. Platau, Phys. Rev. Lett. **45**, 1597 (1980).
[36] T. Gouder, F. Wastin, J. Rebizant, and L. Havela, Phys. Rev. Lett. **84**, 3378 (2000).
[37] J. Terry, R. K. Schulze, J. D. Farr, T. Zocco, K. Heinzelman, E. Rotenberg, D. K. Shuh, G. van der Laan, D. A. Arena, and J. G. Tobin, Surf. Sci. **499**, L141 (2002).
[38] H.-D. Kim, H.-J. Noh, K. H. Kim, and S. J. Oh, Phys. Rev. Lett. **93**, 126404 (2004).
[39] J.-C. Griveau, J. Rebizant, G. H. Lander, and G. Kotliar, Phys. Rev. Lett. **94**, 097002 (2005).
[40] A. J. Arko, J. J. Joyce, L. Morales, J. Wills, J. Lashley, F. Wastin, and J. Rebizant, Phys. Rev. B **62**, 1773 (2000).
[41] J. Naegele, *Numerical Data and Functional Relationships in Science and Technology*, Landoldt-Börnstein, New Series, Group III, Vol. 23, pt. b (Springer-Verlag, Berlin, 1994), p. 300.
[42] M. B. Brodsky, A. J. Arko, A. R. Harvey, and W. J. Nellis, in *The Actinides: Electronic Structure and Related Properties*, edited by A. J. Freeman and J. B. Darby, Jr. (Academic, New York, 1974), Vol. II, pp. 185–264.
[43] J. G. Tobin, K. T. Moore, B. W. Chung, M. A. Wall, A. J. Schwartz, G. van der Laan, and A. L. Kutepov, Phys. Rev. B **72**, 085109 (2005).
[44] K. T. Moore, G. van der Laan, R. G. Haire, M. A. Wall, and A. J. Schwarz, Phys. Rev. B **73**, 033109 (2006).
[45] While some covalency may occur in both oxides, the predominant configuration appears established. See, K. N. Kudin, G. E. Scuseria, and R. L. Martin, Phys. Rev. Lett. **89**, 266402 (2002) for UO_2 and L. Petit, A. Svane, Z. Szotek, and W. M. Temmerman, Science **301**, 498 (2003) for PuO_2.
[46] P. M. Oppeneer, T. Kraft, and M. S. S. Brooks, Phys. Rev. B **61**, 12825 (2000).
[47] L. Petit, A. Svane, W. M. Temmerman, and Z. Szotek, Eur. Phys. J. B **25**, 139 (2002).
[48] L. V. Pourovskii, M. I. Katsnelson, and A. I. Lichtenstein, Phys. Rev. B **72**, 115106 (2005).
[49] P. Wachter, F. Marabelli, and B. Bucher, Phys. Rev. B **43**, 11136 (1991).
[50] A. O. Shorikov, A. V. Lukoyanov, M. A. Korotin, and V. I. Anisimov, Phys. Rev. B **72**, 024458 (2005).
[51] The technique of resonant inelastic x-ray scattering appears to hold the most promise—see the work on Ce; J.-P. Rueff, J.-P. Itie, M. Taguchi, C. F. Hague, J.-M. Mariot, R. Delaunay, J.-P. Kappler, and N. Jaouen, Phys. Rev. Lett. **96**, 237403 (2006).
[52] A. B. Shick, L. Havela, J. Kolorenč, V. Drchal, T. Gouder, and P. M. Oppeneer, Phys. Rev. B **73**, 104415 (2006).
[53] A. Landa and P. Söderlind, J. Alloys Compd. **376**, 62 (2004).